**The Magnetic and Electrical Properties of**

**Permalloy-Carbon Thin Film Multilayers**

A thesis submitted in partial fulfillment of the requirement
for the degree of Bachelor of Science with Honors in
Physics from the College of William and Mary in Virginia,

by

Heather A. Faltin

Accepted for

_____

(Honors, High Honors, or Highest Honors)

_____

Director

Dr. Anne Reilly

_____

_____

_____

Williamsburg, Virginia
**April 2000**

## Table of Contents


I. Introduction
II. Theory
  A. Ferromagnetism
  B. Domain Structure
  C. Resistivity and Giant Magnetoresistance
  D. Carbon Thin Films
  E. Issues in Magnetic Multilayer Thin Film Growth
III. Experimental Procedures
  A. Permalloy-Carbon Multilayer Samples
  B. Scanning Electron Microscopy
  C. Atomic and Magnetic Force Microscopy
  D. Vibrating Sample Magnetometry
  E. Van der Pauw Resistivity Measurements
  F. Carbon Samples
IV. Results
  A. Scanning Electron Microscopy
  B. Atomic Force Microscopy
  C. Magnetic Force Microscopy
  D. Vibrating Sample Magnetometry
  E. Resistivity
V. Conclusion

Acknowledgements

This project would not have been possible if it had not been for the help of many people. My sincere thanks go to my advisor, Dr. Anne Reilly. I do not know what I would have done without her guidance and expertise. I was inspired by her excitement for our research and I only hope that she enjoyed working with me at least half as much as I enjoyed working with her.

I would also like to take a moment to thank the people who generously donated their time to create samples and run experiments. Many thanks go to Dr. Brian Holloway in the Applied Science Department for use of his sputtering chamber and some of his carbon nitride films. His knowledge and expertise in the field of carbon thin film deposition was critical to this work. Also thanks to Jason Gammon who helped grow the amorphous carbon samples used in this project.

Jewel Thomas in the Biology Department instructed me on how to use the Scanning Electron Microscope. Her patience and sense of humor were greatly appreciated.

Finally, I would like to thank Dr. Buzz Wincheski for allowing me access to the Vibrating Sample Magnetometer and the Atomic and Magnetic Force Microscope located at NASA-Langley. Without his help and very generous donation of time and effort, the most important results would never have been obtained.

**Abstract:**

Magnetic thin film multilayers are incredibly useful to today's technology, especially in regard to magnetic memory data storage and improved computer hard disk drives. The incorporation of carbon as the nonmagnetic layer may be the next step in thin film multilayer technology because of its electrical and mechanical properties. This project explores the properties of carbon-magnetic thin films. The results indicate that amorphous carbon has little negative impact on the magnetic properties of permalloy, while carbon nitride causes an increase in coercivity, roughness, and resistivity.

## I. Introduction

Within the last decade the world has undergone a technological revolution due to the rapid increase in computer capabilities. The explosion of the internet has changed the way business is conducted, governments are run, and relationships are maintained. In many ways, technology developed in the last decade of the twentieth century fostered great social and economic change through the entire world.

Many of these advances would not have been possible had it not been for the discovery and implementation of technology known as magnetic thin film multilayers. These devices consist of thin, alternating layers of non-magnetic and ferromagnetic materials, where each layer is only several nanometers ($10^{-9}$m) thick. The nonmagnetic layer can consist of metals, such as copper, or ceramics, such as $Al_2O_3$. Common ferromagnetic materials include iron, cobalt, nickel, and alloys such as permalloy (NiFe). A common thin film multilayer used as a computer hard drive sensor consists of layers of permalloy and copper. The technological applications of these materials revolve around their capacity to sense magnetic fields and store memory.

The most notable property of magnetic thin film multilayers is giant magnetoresistance(GMR), which is defined as the large change in resistance experienced by the thin film multilayer in an applied magnetic field. This change in resistance has been measured to be up to 220%[1]. It is this property that makes these multilayers such sensitive magnetic field sensors. GMR was discovered in 1988 by

Albert Fert and colleagues in France[2] and its discovery has led to incredible increases in computer memory storage capabilities.

To provide insight into the impact of these films, consider the history of the computer hard drive. Invented in the 1950s, the first computers stored approximately five megabytes of memory within a structure the size of a large refrigerator. Memory was expensive, costing tens of thousands of dollars per megabyte. In 1991, with the invention of the first read head using magnetic thin film technology, computers were able to store gigabytes of information in a structure weighing about two pounds and costing about two dollars per megabyte[3].

While the breakthroughs made possible by the enormous increase in memory capacity is a feat unto itself, the economic impact of magnetic thin films is equally startling. In 1997, IBM announced the first read heads based on GMR in magnetic thin films for magnetic hard disks. Economically, the market for these products ranges to about one billion dollars per year. An even stronger financial impact is anticipated as researchers work to develop nonvolatile magnetic memory storage, which has the potential to revolutionize the random access memory (RAM) market. At present, the RAM market exceeds one hundred billion dollars annually.[4]

To store memory, a hard drive exploits the magnetic properties of these multilayers. Data is stored on a hard drive in areas known as bits, which utilize magnetic domain structures. A domain is a region of magnetic material having only one direction of magnetization. Orientation of a domain in one direction represents a "one," while orientation in the opposite direction represents a "zero." When a sensor, or read head, runs over the bits on the disk, it senses the small changes in magnetic

field. Read heads using GMR magnetic thin films show a large change in resistance with even the small change in the magnetic field presented by the bits on the hard disk. Because the resistance changes across the read head, an electrical signal relayed from the read head to the CPU changes, enabling the binary code of zeros and ones to be transmitted. In this manner, data stored on the disk is conveyed to the computer.

While already impressive, many challenges still face the field of magnetic thin film multilayers. One area of research explores improved growth techniques that would allow accuracy of thickness down to the angstrom level. Controlling growth to this level may increase the GMR effect. Research is being conducted to improve film durability and to also discover new, cheaper materials. All of these would have direct implications for the computer market; thinner, more durable films would allow for more sensitive read heads that could be brought closer to the hard disk. Another area of interest is the development of biocompatible thin films that could be used for medical applications.

This project strives to meet some of these goals through the growth and characterization of carbon-magnetic multilayers. With carbon being an inexpensive, durable, and structurally diverse material with obvious biocompatible characteristics, it may be an ideal candidate for use as the non-magnetic layer in a multilayer device. One interesting feature of carbon is that its properties vary widely depending upon the bonding hybridization. Hard carbon films are those displaying diamond-like properties. Soft carbons are more similar to graphite. For example, the low coefficient of friction and high thermal conductivity of hard carbon films indicates potential value to the computer industry.

In this project, a ferromagnetic thin film (permalloy) is deposited on top of two types of carbon and the structural, magnetic, and electrical properties of the permalloy thin films are explored. This project explores the characterization of the magnetic properties of carbon-magnetic multilayers. The techniques used are: scanning electron microscopy, atomic and magnetic force microscopy, vibrating sample magnetometry, and Van der Pauw resistivity measurements. The results of these experiments will help our understanding of how depositing a magnetic multilayer on top of a carbon layer affects the structural, magnetic, and electronic properties of the magnetic layer. This is the first step that must be taken to determine if carbon and ferromagnetic films can be combined into a useful multilayer. It is desired that the growth of the ferromagnetic layer with carbon will not negatively impact the properties of the ferromagnetic layer.

## II. Theory

The usefulness of magnetic multilayer thin films derives from a phenomenon known as giant magnetoresistance (GMR). GMR is the large increase in resistance across a magnetic multilayer when that multilayer is in the presence of an applied magnetic field. Placed in a changing external magnetic field, the device will show large changes in resistance, on the order of one hundred to two hundred percent, making this a very sensitive magnetic field sensor.

This project attempts to grow and characterize carbon-magnetic multilayers. To understand the process and results of the experiments, it is necessary to understand the basic physical principles involved. The concepts of ferromagnetism, domain structure, and resistivity are crucial to the development of thin films. The quantum mechanical process of spin-dependent transport is necessary to explain the phenomenon of giant magnetoresistance. Finally, a review of carbon compounds will enhance the reader's understanding of the growth and properties of these materials.

### *A. Ferromagnetism*

Magnetic materials are traditionally grouped into three categories: diamagnetic, paramagnetic, and ferromagnetic. Ferromagnetic materials are the most useful to thin film technology because of their nonvanishing magnetic moment. Unlike paramagnetic and diamagnetic materials, ferromagnets exhibit a magnetic moment even in the absence of an external magnetic field[5]. The most

common elemental ferromagnets are the 3d transition elements nickel, cobalt, and iron.

Magnetization is defined as the magnetic moment per unit volume and, for iron, cobalt, and nickel, results from the unpaired spin of electrons in the 3d orbital. According to the Pauli Exclusion Principle, no two electrons can occupy the same state, or more explicitly, no two electrons can have the same quantum numbers. Electrons fill orbitals according to Hund's Rules, which relate total spin of the electrons to the energy of the whole. Since nature always favors a state of minimum energy, electrons choose the spin configuration that yields lowest energy. In most simple cases, Hund's Rules lead to antisymmetric spin states. For example, if the first electron has spin +1/2, the next electron will occupy the orbital with spin –1/2.

In the case of cobalt, iron, and nickel, this is not so. Energy in the ferromagnetics is minimized by parallel, rather than antiparallel, spin alignment because of the impact of "exchange energy." The net electronic wave function of a two electron system can be described by:

$$\Psi = y_1(R_1)y_2(R_2) - y_2(R_1)y_1(R_2) \qquad (1)$$

The total energy over a volume,$\tau$, includes the terms:

$$\int y_1^*(R_1)y_2^*(R_2)y_1(R_1)y_2(R_2)\frac{e^2}{r_{12}}dt \qquad (2a)$$

$$-\int y_1^*(R_2)y_2^*(R_1)y_1(R_1)y_2(R_2)\frac{e^2}{r_{12}}dt \qquad (2b)$$

$$-\int y_1^*(R_1)y_2^*(R_2)y_1(R_2)y_2(R_1)\frac{e^2}{r_{12}}dt \qquad (2c)$$

$$+\int y_1^*(R_2)y_2^*(R_1)y_1(R_2)y_2(R_1)\frac{e^2}{r_{12}}dt \qquad (2d)$$

where $\psi$ represents the quantum mechanical wavefunctions of electrons 1 and 2, and $R_1$ and $R_2$ represent their positions prescribed by R. The equations 2a and 2b above both contain the terms $y_1^*(1)y_1(1)$ and $y_1^*(2)y_1(2)$ which indicate that they represent the Coulomb interaction energy.[6] As (2b) and (2c) above do not contain these terms, they must represent some other energy, namely the exchange energy.

Exchange energy is represented by:

$$w = -2\vec{J}_K \vec{S}_i \bullet \vec{S}_j \qquad (3)$$

where $S_i$ and $S_j$ are the spin vectors and $J_k$ is known as the "exchange integral." The value for $J_k$ is usually negative, thus the exchange energy is positive unless $S_i$ and $S_j$ are oppositely directed. This explains why antisymmetric spin states are usually favored. $J_k$ becomes positive when the ratio of interatomic distance to the radius of the unfilled shells exceeds three. When $J_k$ turns positive, the minimum exchange energy is obtained when the spin vectors are parallel to each other. This ratio is indeed greater than three in the case of iron, cobalt, and nickel.

Thus, as nature tries to minimize energy, the parallel spin states are favored. These parallel spin states combined create a net magnetic moment for the entire material. This explains why ferromagnetic materials have a net magnetic moment even in the absence of an external magnetic field.

*B. Domain Structure*

A domain is a region of magnetic material having only one direction of magnetization. Any structure larger than one one-hundredth of a millimeter in size will have at least one domain.[7] Domains are useful to the computer industry as each unit of memory, or bit, is in essence a domain. In this project, magnetic multilayers with few but clearly defined domains are the goal.

Domains are formed to decrease the energy stored in the external field created by the magnetic device. Magnetostatic energy is described by:

$$W = \int_{-\infty}^{+\infty} B^2 dt \qquad (4)$$

where B is the magnetic field created by the magnet. Domains will form until the energy needed to create a domain wall equals the decrease in energy obtained by the surrounding field.[8]

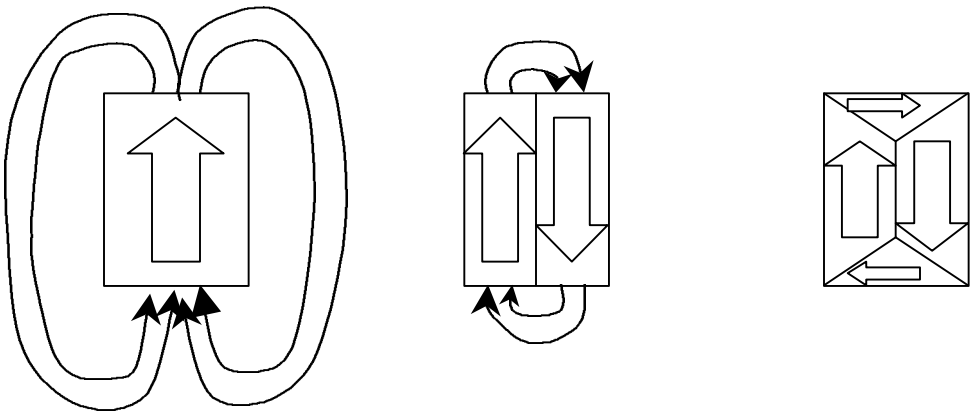

**Figure 1: Domain Formation. Domains form in order to minimize the magnetic field and thus the magnetic energy.**

The leftmost diagram in Figure 1 shows one domain. To reduce energy stored in the field, two domains form, as the middle diagram represents. To further reduce energy, the domains split again as in the third diagram.

An interesting result of domain structures is a phenomenon known as hysteresis. Generally, hysteresis is the notion that the magnetization of a magnet in an applied field is not solely a function of the applied field, but also of the history of the magnet. A hysteresis loop plots magnetization versus applied magnetic field. As the applied magnetic field is raised from zero (labeled A in Figure 2) the magnetization increases until it reaches saturation(B). After saturation, no change in magnetic field will increase the magnetization of the sample(C). As the field is decreased, the magnetization also decreases, but following a different path through (D). Again, the magnetization will decrease until negative saturation(E). If one were to increase the applied field again, the magnetization would again increase, but following a still different path, through (F). The width of the hysteresis loop indicates the coercivity of the sample. The coercive force is the field necessary to restore zero magnetization from saturation.(D,F)[9]

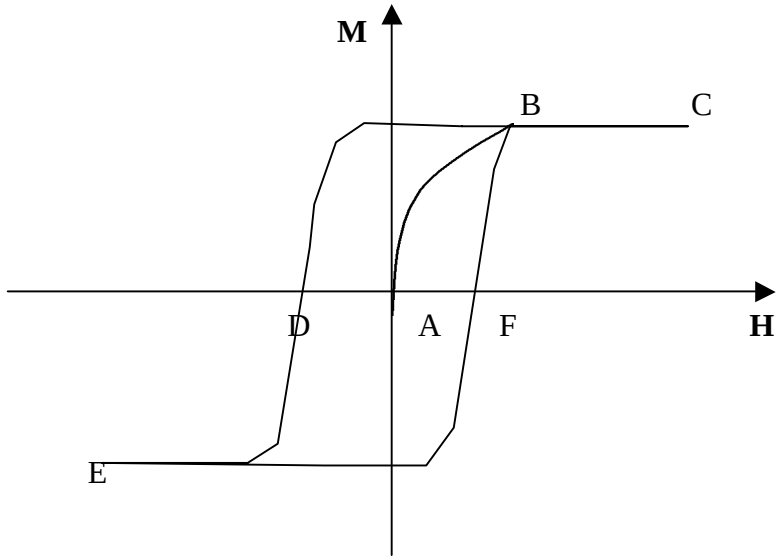


**Figure 2: A hysteresis loop plots magnetization(M) vs. applied magnetic field (H) for a ferromagnetic materials displaying hysteresis.**

Hysteresis results from the shifting of domain walls. As the material becomes magnetized, the domains reorient themselves. In a weak field, the shifts are small and reversible. In a strong field, imperfections in the structure obstruct domain wall movement. The walls will pass this imperfection only when the gain in energy is significantly large. As these imperfections prevent magnetization, they also hinder the walls from returning to the original state, which explains the varying paths upon magnetization and demagnetization. At saturation, the domain walls have shifted the maximum amount and all that is left is one single domain which rotates to be parallel with the applied field. No further increase in magnetic field increases the magnetization after this.

The fact that hysteresis is related to structural imperfections is important to the growth and characterization of magnetic multilayers. Even perfect crystalline ferromagnetic thin films will have domains and a hysteresis curve which is determined by the orientation of the crystal relative to the applied

field. In general, as defects are introduced into the crystal, domain walls become pinned on these defects and the coercivity increases. Such defects include impurities and interruptions in the crystalline structure. Thus, for magnetic sensor applications, where low coercivity is desired, thin films free of many structural defects is required.

*C. Resistivity and Giant Magnetoresistance*

Giant magnetoresistance is the most important quality found in magnetic multilayer thin films. It is defined as the large change in resistance in magnetic multilayers in an applied field. The resistance changes are frequently on the order of one hundred to two hundred percent and are due to spin-dependent transport.

Resistivity is determined by the scaterring of electrons. The more scattering, the higher the resistance.[10] In order for an electron to scatter, there must be an allowed energy state for it to occupy. Therefore, the availability of unoccupied states is the key determinant for the resisitivity of materials.

According to Mott, electrical conduction can be thought of as occuring through the two spin channels, spin +1/2 or spin –1/2, or up and down. Up and down are defined relative to the direction of magnetization. In non-ferromagnetic materials such as copper, there is no difference in the energy band structure for up and down spins, so there is no difference in resistivity for up and down spins. For a ferromagnet such as Co, Ni or Fe, however, the "spin-up" state, meaning the state in which the electrons all have their spin

oriented in the same direction, is favored because of the exchange energy, as previously discussed. Therefore, the spin-up state for 3d electrons in ferromagnets is completely filled, while the spin-down state is only partially filled. Electrons moving through the material polarized in the spin-down state will have the ability to scatter freely because there are available spin-down states for them to scatter to. This means the resistivity for this spin state will be high (see Figure 3). On the other hand, electrons polarized in the spin-up state will have a lessened ability to scatter because all of the spin-up states are filled, ensuring that the resisitivity for this spin state is low. In magnetic multilayers, this scattering effect is repeated through each layer, which amplifies the effect on resistivity.

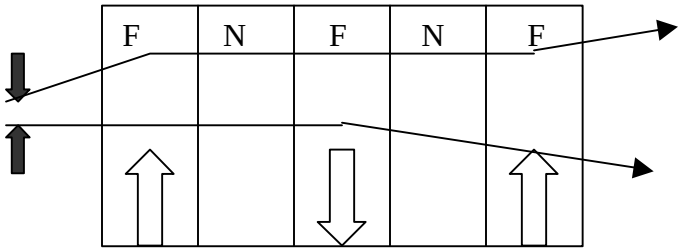


Antiparallel State: Resistance is high

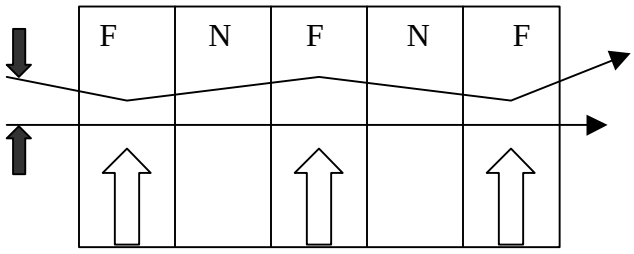


Parallel State: Resistance is low

**Figure 3: A simple phenomenological picture of the source of GMR in magnetic multilayers. Scattering in magnetic multilayers causes resistance to increase. F represents a ferromagnetic layer. N represent nonmagnetic layer. The open arrow in the F layers indicates the direction of magnetization. The black arrows indicate the direction of the electron spin. "X's" indicate scattering events.**

*D. Carbon thin films*

Carbon is a very interesting material because its properties can range from graphitic to diamond-like depending on its atomic bonding. Graphitic carbon is highly electrically conductive and is relatively soft while diamond is hard and is an excellent insulator.

In graphitic carbon, there are four bonds from the hybridization of the 2s and 2p shells into three $sp^2$ bonding orbitals and an unfilled 2p orbital. In the case of diamond, the valence electron shells hybridize into four $sp^3$ bonding

orbitals equidistance from each other. In diamond there are no unfilled hybrid or ground state orbitals, so there is no pi bonding[11]. The famous tetrahedral shape and the strong sigma bonds of the diamond molecule is what creates its strength and durability.

Because the properties of carbon can be controlled over such a wide range depending upon how it is grown, it is a very interesting material for thin-film applications. Two forms of carbon thin films are used in this project: amorphous carbon and carbon nitride. Amorphous carbon is a general term which refers to carbon with a mixed degree of $sp^2$ and $sp^3$ bonding. The amorphous carbon we use in this project is probably closer in properties to graphite. Carbon nitride is a hard carbon material and interest in it stems from its properties which mimic those of diamond such as a low coefficient of friction and strong durability.

Research has shown that the coefficient of sliding friction of carbon nitride films was in fact superior to that of diamond like carbon when tested on magnetic disks. The coefficient of sliding friction for carbon nitride was 0.2, while diamond-like carbon rated at 0.4.[12] The same researchers also found that carbon nitride has a wear life of three to four times greater than diamond-like carbon.[12] These qualities make carbon-nitride a material worthy of future investigation.

*E. Issues in Magnetic Multilayer Thin Film Growth*

Magnetic thin films are commonly grown by a technique called sputtering, in which atoms are liberated from a target by being bombarded by argon ions and then deposited onto a substrate (see description of sputtering in Section IIIA). When sputtering one material (such as Ni) onto another material (such as amorphous carbon), there are several considerations. First, one is concerned about the overall crystalline structure of the layers. The bottom layer might not grow in a crystalline fashion (such as amorphous carbon) and may hinder the growth of crystalline material on top of it, although this is not always the case.

Other issues to consider are the roughness of the resulting films and the intermixing between the different layers. Sometimes the film which grows does not grow in a perfectly smooth manner, but has a certain amount of roughness. There is also the possibility of intermixing one layer with another. This is more of a problem the higher the momentum of the sputtered atoms, and also if the substrate is heated. The amount of roughness and intermixing is dependent on sputtering parameters such as gas pressure, deposition rate and substrate temperature.

For magnetic thin films, roughness may present a problem. Roughness in one layer may create effect in the crystallinity of the next layer. For a polycrystalline film (one which is made up of regions of crystallinity called grains), roughness may affect the size and orientation of the grains (the

magnetic layer in our films is believed to be polycrystalline). This can have a negative effect on magnetic properties and resistivity. When the magnetic layer is sputtered upon the rough nonmagnetic layer, it can land in the crevices of the rough nonmagnetic material. This disrupts magnetization and may create a dead layer. A dead layer is a region of a ferromagnetic thin film where the magnetization is greatly decreased. For intermixing, the elements of the two layers actually intermix and sometimes form a chemical species, such as NiC (nickel carbide) in Ni/C multilayers. NiC has a decreased magnetization relative to Ni, and its formation may also lead to a dead layer. The group of Krishan *et al*. has studied multilayers of Fe/C, Ni/C and Co/C (stacks of about 100 layers each), where the carbon was amorphous. They found for Ni and carbon, a dead layer consisting of NiC was formed for about 15 angstroms.[13] Intermixing may also increase the resistivity of the material by providing more scattering sites.

## III. Experimental Procedures

In this project, permalloy (NiFe) ferromagnetic thin films were deposited on top of carbon thin films. Characterization of these magnetic multilayers devices involved the use of five experimental procedures. Scanning Electron Microscopy(SEM) was used to image the surface. Atomic Force Microscopy(AFM) was used to map the topography of the surface. Surface roughness and grain size are important because of their impact on domain formation. Magnetic Force Microscopy (MFM) is also used in this project for its ability to map the domain structure of the sample. Vibrating Sample Magnetometry (VSM) was used to generate a hysteresis loop for the different films that were grown, and to determine the relationship between sample thickness and magnetization. Finally, resistivity was determined using the Van Der Pauw method. Also discussed is the growth of the carbon films through sputtering.

### *A. Carbon-Permalloy Samples*

Carbon is a highly useful and versatile material. It can range from the soft graphitic carbon to the diamond structure, which is the hardest substance known in the world. Amorphous carbon and carbon nitride samples were used in this project. The amorphous carbon grown in this project is most similar to graphite, so it is a soft carbon material while carbon nitride is a harder carbon.

The amorphous carbon was deposited onto ½ inch by ½ inch silicon substrates via sputtering in a single-target sputtering chamber located in the Applied Science Department. Jason Gammon grew 16 amorphous carbon samples for this project using a sputtering chamber and with the substrate at room temperature, with assistance of the author. We used a 3 inch circular graphite target for sputtering and deposited it in an argon environment with the substrates at room temperature and vacuum pressures in the mTorr regime. The amorphous carbon films were approximately 3 micrometers thick, determined by SEM by Brandt Robertson at the Applied Research Center.

A sputtering chamber consists of a vacuum chamber fitted with a target of the material to be sputtered, and a substrate on which the film will be grown. First, the chamber is evacuated to pressures less than $1x10^{-5}$ Torr and then refilled with argon gas. A large negative voltage is applied to the target, which causes the argon gas to form a plasma of positive ions. A magnetic field around the target traps the ions and causes them to move in a circular pattern around the target. The ions are then accelerated into the target due to its negative potential. By conservation of momentum, particles of the target material, in this case carbon, fly across the sputtering chamber and land upon the silicon substrate. There is a potential difference between the target and the substrate that accelerates the movement of particles between the target and the substrate.

Changes in chamber conditions facilitate the formation of different carbon structures. The room temperature conditions allowed amorphous carbon to

grow. The one carbon nitride sample used in this study was grown by Dr. Brian Holloway at Stanford University following a similar method, only at a higher temperature (>400° C) and in a nitrogen environment.

The ferromagnetic layer, consisting of permalloy (80%Ni, 20% Fe) was deposited onto the carbon films by Reza Loloee at Michigan State University in a 50 mTorr argon environment and substrates at approximately room temperature. The sputtering guns at MSU were capable of depositing a ferromagnetic material. The thickness of the permalloy films were determined at MSU by use of a crystal film thickness monitor in the sputtering chamber. All the permalloy samples were then coated with 5nm of Nb to protect the permalloy layer.

We initially attempted to deposit the ferromagnetic material in the same sputtering chamber in which the amorphous carbon was grown. This was attempted by placing a ferromagnetic target (initially Fe) in the sputtering chamber. We were unsuccessful, however, because the magnetic field from the target disrupted the magnetic field of the sputtering gun which traps the argon ions. We were unable, therefore, to sustain an argon plasma, regardless of how thin we made the ferromagnetic target.

### *B. Scanning Electron Microscopy*

A scanning electron microscope is analogous to an optical microscope, but instead of light it uses electrons to image. The advantage of electrons is that

their de Broglie wavelength(ë=h/p) is on the order of 10 Å, much less than that of light. This allows smaller features to be imaged[14].

A scanning electron microscope takes pictures of the surface of a specimen by sending an electron beam across its surface. A detector measures the current from the electron beam that is reflected, and also the current from the secondary electrons excited off of the specimen by the incident electrons[15]. The current is interpreted into a visual picture on a monitor. Characterization of the roughness of the films is crucial, since this affects the magnetic and electronic properties of the multilayers. The SEM used in this study was located in Millington Hall.

*C. Atomic and Magnetic Force Microscopy*

This project used the Digital Instruments Multimode Scanning Probe Microscope (MSPM), located at NASA-Langley, which has the capabilities of both an atomic and magnetic force microscope. In atomic force microscopy, a small tip, which is on the order of one hundred angstroms wide, is located at the end of a cantilever and dragged over the surface of the sample. At this level, van der Waals forces dominate. As the tip moves up and down over the surface, a laser beam is directed at the tip. The reflection is monitored by a photosensor. The topography is traced out as the sensor detects the reflection.

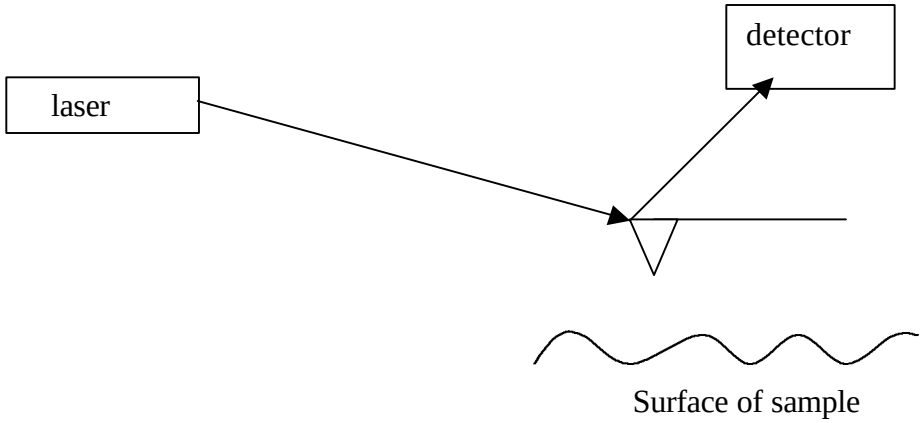


**Figure 4: Diagram illustrating the concept of AFM and MFM. A laser is directed on to the cantilever and its reflection is measured by the photodetector, For MFM, the tip is raised off the surface of the sample and deflected by magnetic forces.**

Magnetic Force Microscopy is based upon the same principles as the AFM except that the tip is coated with a ferromagnetic material. The tip, which is raised above the surface of the sample so as not to touch it, is deflected by the magnetostatic repulsion generated by the interaction between the magnetized tip and the magnetic sample.

To avoid problems involved with accidental tip contact with the surface in MFM mode, the Digital Instruments MSPM is slightly more complicated in design. Digital Instruments employs a procedure known as LiftMode™. In this mode, for each raster of the scanning pattern, the sensor makes two passes across the sample. On the first pass, topographical AFM data is gathered as the tip gently taps across the surface. On the second pass, this topographical information is used as the tip lifts 10 to 100nm off the surface and follows the topographical pattern determined in the first pass. This ensures that the tip will not accidentally crash into the surface, which would damage the instrument and skew the data.

To improve the resolution of the MFM data, the Digital Instruments MSPM does not rely solely upon the deflection of the tip by magnetic forces. Instead, the tip oscillates at a resonant frequency of approximately 100 kHz and amplitude between 10 and 100nm. The magnetic field generated by the sample alters the spring constant (k) which therefore shifts the tips resonant frequency:

$$\Delta f_0 = \frac{f_0}{2k} F' \qquad (5)$$

where F' is the vertical component of the force exerted on the tip, assuming the tip has a magnetic dipole oriented in the vertical direction and magnetization $\vec{m} = m\hat{z}$. F' can be described by:

$$F_z' = \int \vec{m}(\vec{r}') \bullet \frac{\partial^2 \vec{B}}{\partial z^2}(\vec{r} - \vec{r}')d^3r' \qquad (6)$$

where H is the stray field from the sample[16].

The shift in frequency is tracked by laser detection as described above and is proportional to the magnetic force. The two pass method allows the simultaneous generation of AFM and MFM images. For the Digital Instruments MSPM, the MFM resolution is 10 nm or better and can register forces as small as $1x10^{-10}$ N[17].

*D. Vibrating Sample Magnetometer*

The VSM used in these experiments was the Lakeshore Model 7300, located at NASA-Langley. A VSM generates a hysteresis loop, or a plot of a sample's magnetization versus the applied field over time. A sample is

placed in a uniform magnetic field created by an electromagnet. The electric field induces a magnetic moment, **m**, in the sample. Next, the sample is made to vibrate sinusoidally. The magnetic flux generated by the vibrating sample induces a current in the pick-up coils. This current is proportional to the magnetization of the sample.

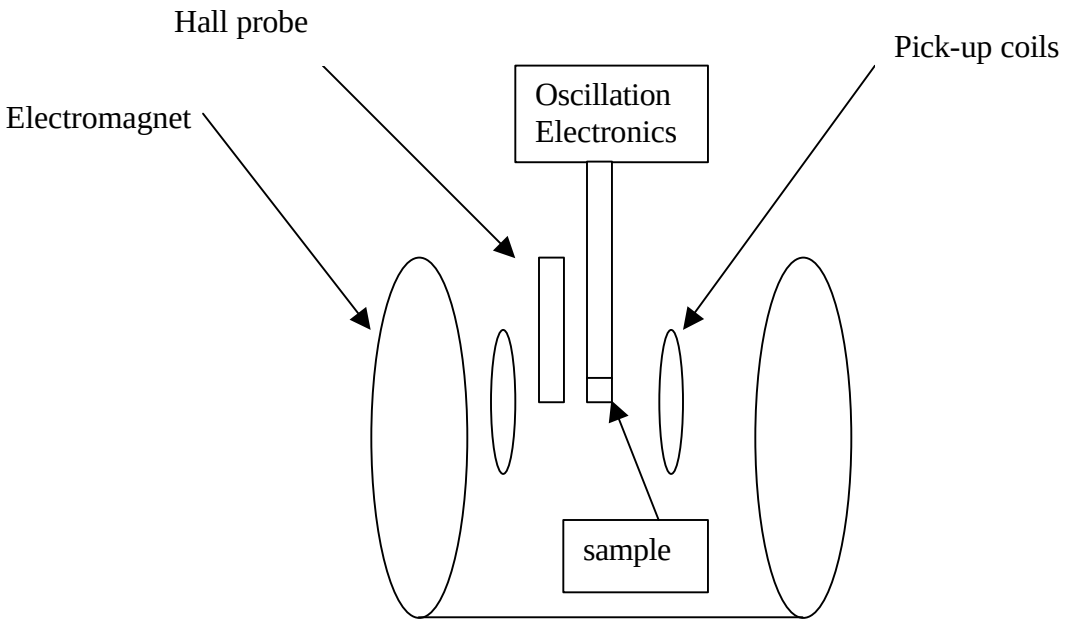


**Figure 5: Diagram illustrating theVibrating Sample Magnetometer Set-Up. The magnetic sample is made to oscillate sinusoidally by the electronics. The vibrating magnetic sample creates a changing magnetic field which in turn induces a current in the pickup coils. The electromagnet changes the applied magnetic field on the sample from positive to negative saturation, enabling the entire hysteresis loop to be determined.**

*E. Van der Pauw Resistivity Measurements*

According to the theory proposed by L.J. van der Pauw, the resistivity and Hall effect of a flat sample of arbitrary shape can be measured without knowing the current pattern if certain conditions exist[18]. These include:

(a) Contacts are at the circumference of the sample

(b) Contacts are sufficiently small

(c) Sample is of homogeneous thickness

(d) Surface is singly connected—there are no isolated holes.

According to Van der Pauw's theory, the resistivity of the multilayer samples, which meet the above criteria, can be determined by applying a voltage across one side of the sample, and reading the corresponding current produced in the other side. Leads were connected to the multilayer thin film samples using indium solder according to the pattern:

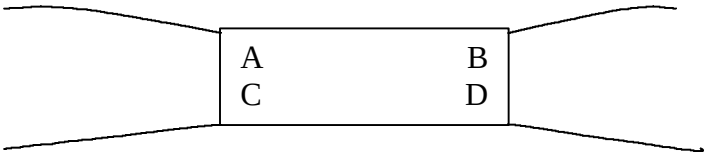


**Figure 6: Leads attached to carbon-magnetic sample for Van der Pauw Resistivity Measurements**

The current was measured using a highly sensitive Keithley Sourcemeter (Model 2400), and the voltage was measured by a Keithly Nanovoltmeter (Model 2182). Using Ohm's Law (V=IR) to determine the resistance across the sample, resistivity can be determined by using the formula:

$$r = \frac{pd}{\ln 2} \frac{R_{AB,CD} - R_{BC,DA}}{2} f\left(\frac{R_{AB,CD}}{R_{BC,DA}}\right) \qquad (7)$$

where f is a function of $R_{AB,CD}/R_{BC,DA}$ and $R_{AB,CD}$ is the potential difference, $V_d$-$V_c$, between D and C per unit current through contact A and B. For measurement of permalloy on carbon, it is assumed that the current is flowing only through the top permalloy layer and not the carbon.

## IV. Results

### A. *Scanning Electron Microscopy*

The scanning electron microscope located in Millington Hall was used to image samples of both amorphous carbon and diamond-like carbon (DLC). Carbon was sputtered on to silicon wafer substrates into the amorphous carbon structure. Brandt Robertson at the Applied Research Center measured the thickness of the sputtered carbon, by an SEM of the substrate edge, to be approximately 3 micrometers. Two of these samples were used for SEM images, while the others were shipped to Reza Loloee at Michigan State University where they were coated with the permalloy to create a carbon-magnetic multilayer. Permalloy films of 5, 10 ,20, 40 ,60 and 120 nm were deposited on amorphous carbon while 120 nm was deposited on the carbon nitride. The permalloy used in this study was composed of 80% nickel and 20% iron. Permalloy is widely used in magnetic thin films.

It was necessary to investigate the structural properties of the amorphous carbon samples to better understand the formation of the permalloy domains. The largest problem facing strong magnetization is the intermixing of layers. When a magnetic material is deposited on a nonmagnetic material, intermixing could create a "dead layer," in which the magnetic particles are so dispersed that their magnetic moments cancel each other, creating an unmagnetized layer. Also of interest is the location of specific deformities. Domains will often grow around structural imperfections.

SEM scans were taken of two amorphous carbon samples. Scans were taken at 11.8x and 20.2x magnification. At this magnification, the boundary between the carbon and silicon was evident by the contrast in color. No other significant structural properties were evident. Scans taken at much higher magnifications (34,400x and 61,500x) yielded similar results. The surface looks very uniform and smooth, which makes it an ideal nonmagnetic material for the multilayers (see Figure 7).

By contrast, the SEM pictures of the DLC revealed a distinct crystalline structure. Images taken at 16,500x and 7,850x show crystal formations on the order of 1 micron wide. This is important because it proves that the SEM is capable of detecting small structural features, and also qualifies our choice of amorphous carbon over DLC as the nonmagnetic layer in the multilayers.

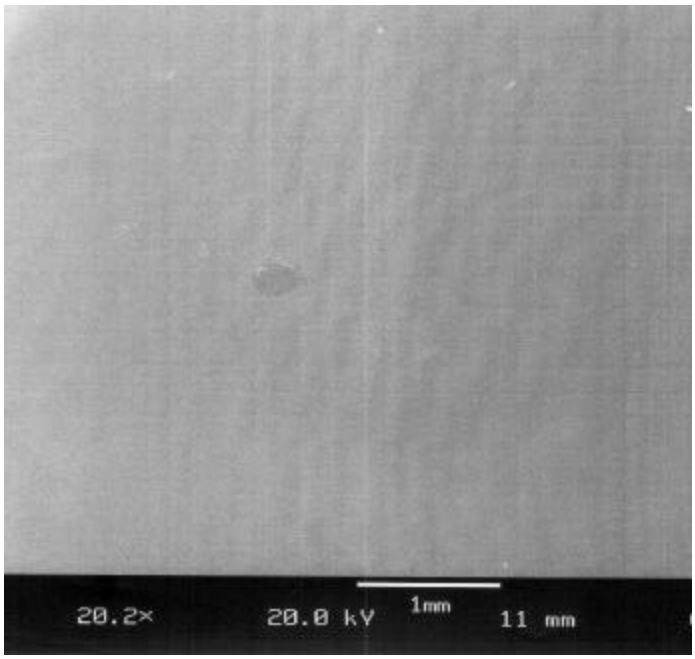

**Figure 7: SEM scan of amorphous carbon. Film is smooth and uniform.**

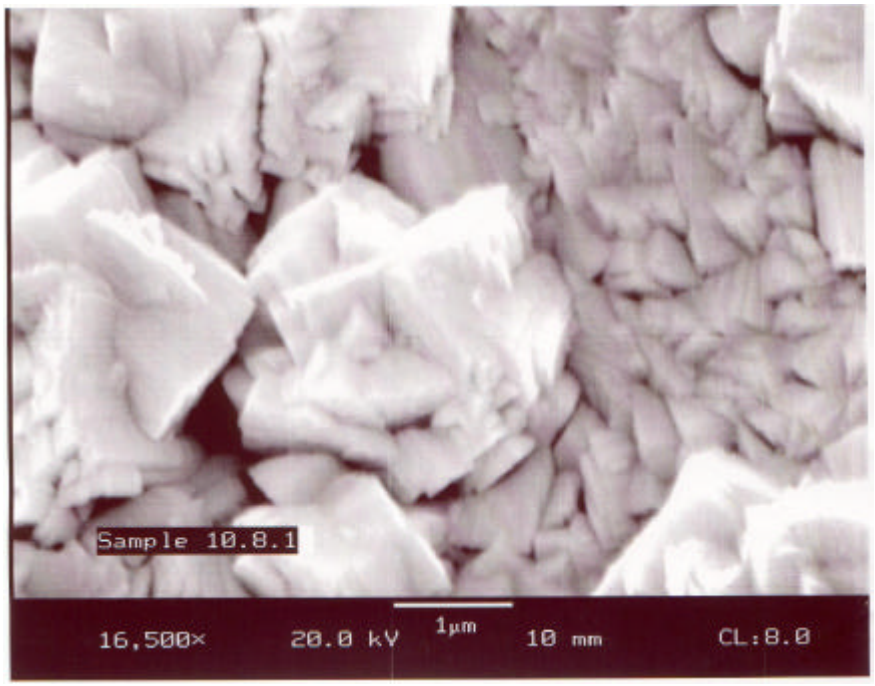


**Figure 8: SEM scan of Diamond Like Carbon.**
**Notice readily visible crystalline structures, on order of 1 micron wide.**

*B. Atomic Force Microscopy*

The samples received from Michigan State consisted of a layer of permalloy of thickness ranging from 5 to 120 nm, on top of a layer of amorphous carbon, on top of a silicon wafer substrate. These samples were scanned by the Digital Instruments MSPM located at the NASA-Langley Research Center in Hampton, Virginia. Also scanned were samples of 120 nm of permalloy on silicon and 120 nm of permalloy on carbon nitride on silicon.

The AFM scans revealed the topography of the permalloy on amorphous carbon samples. Again, the topography seemed smooth, with an average RMS

roughness on the order of 1 nm. The computer program for the AFM calculates the range of heights and the root mean square (RMS) values for the height. These are given as Z range and RMS in Table 1 for the different samples.

As seen in Table 1, the RMS roughness of the permalloy is about 1 nm both on the silicon and amorphous carbon. On the carbon nitride, however, the roughness is significantly larger. The permalloy on CN showed the roughest surface(see Figure 9). Based on approximations judging from the AFM scans, the average grain size is on the order of 400 nm for the carbon nitride, and 100 nm for the permalloy on carbon.

**Table 1**

**Roughness analysis from AFM scans. Numbers given were calculated by the Digital Instruments MSPM analysis software.**

| Sample | Z range (nm) | RMS (nm) |
|---|---|---|
| 10 nm of NiFe on silicon | 5.432 | 0.506 |
| 120 nm of NiFe on silicon | 6.638 | 0.800 |
| 10 nm of NiFe on amorphous carbon | 7.595 | 0.946 |
| 120 nm of NiFe on CN | 270.1 | 19.3 |

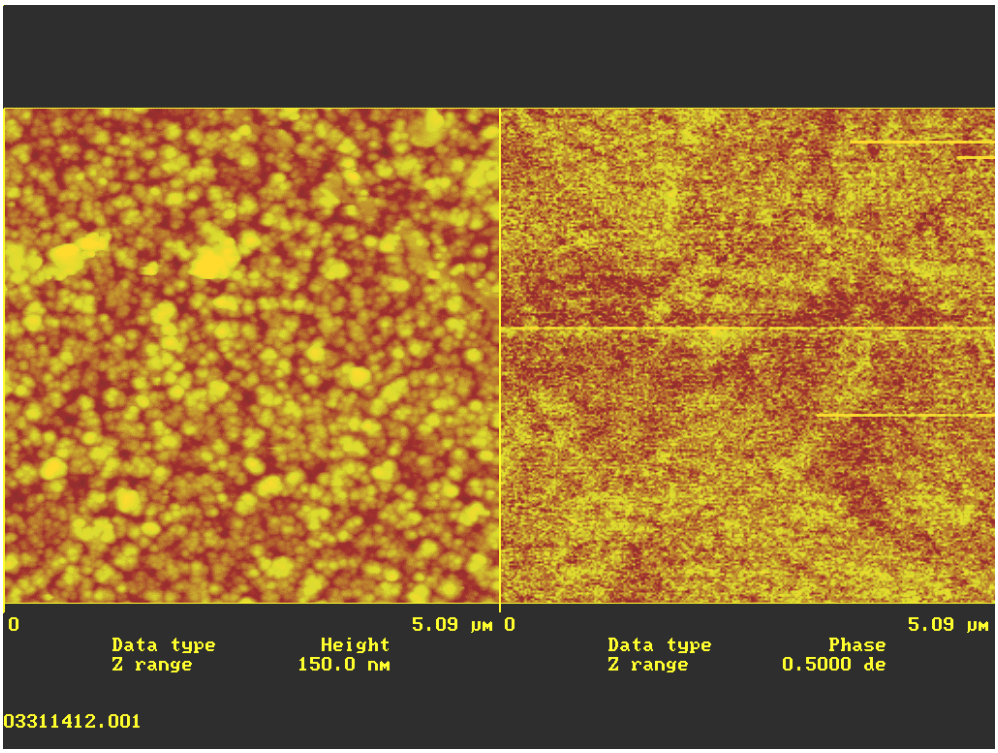


**Figure 9: 5 micron AFM/MFM scan of 120 nm permalloy on CN. AFM is on the left, MFM on the right.**

C. *Magnetic Force Microscopy*

MFM scans were taken of the same samples as the AFM, since the two measurements are taken simultaneously, as described in part III. Scans sizes ranged from 2.2 to 50 µm. Unless we serendipitously landed the tip at the edge of a domain, no domain walls were obvious in the entire scan range. Permalloy thin films deposited upon silicon, amorphous carbon, and CN were all scanned. It was very difficult to see clear evidence of domain contrast or domain walls. Domains were only clearly imaged for a 50 µm scan of 120 nm permalloy on silicon which revealed a bow-tie shaped domain structure (see Figure 11). The corresponding AFM showed a deep hole, about 132 nm deep, in the surface.

There are two reasons for the difficulties we had imaging domains in permalloy using MFM. The first reason is that the average domain size in a permalloy thin film is larger than the scan size. As previously mentioned, domains often form around structural imperfections. In a paper by C. Merton[19], domain formation in permalloy was explored. The researchers studied films with a 20 nm layer of permalloy(81% Nickel, 19% iron) with holes of 10, 5, and 3 ìm patterned into the center. Using the same Digital Instruments equipment as used in this project, 20 ìm scans were taken of the surface. The magnetization around the holes was tangential to the surface of the hole forming a domain wall. In the surrounding area, however, there was only one direction of magnetization. This indicates that the domain size for permalloy in the absence of structural imperfections is larger than 30 ìm.[20] The maximum scan size used in this project is 50 ìm. It is possible that our scans are in the middle of a large domain and so we cannot see the domain walls. Any larger scan would sacrifice sensitivity and thus would not prove any more effective at imaging domains.

The second reason it is difficult to image permalloy domains is due to limitations in our equipment. Originally, we were scanning the sample with a high-moment, high-coercivity magnetic tip. With this tip, some “rippling” structures were seen in the MFM scan (see Figure 10), but no clear evidence of sharp domains or domain walls. We then switched to a low-moment, low-coercivity tip because the high-moment tip may have been affecting the magnetization of the soft permalloy. Domains were still difficult to image even

with this tip. Only around a hole was there clear evidence for domains. Also, the sample mount was held in the microscope by a magnetic mounting plate, although it seemed that the amount of magnetic field at the actual sample was small. Large stray magnetic fields could cause the low-moment permalloy to reach magnetic saturation.

The fact that domains and domain walls could not be imaged on the permalloy on silicon, permalloy on amorphous carbon, or the permalloy on carbon nitride except around a strong structural defect such as a hole (see Figure 11) indicates that the carbon layers are not causing the permalloy to form domains smaller than we are able to image. It is encouraging that the permalloy is not breaking up into significantly smaller domains, although a different domain imaging technique should be used to confirm this result.

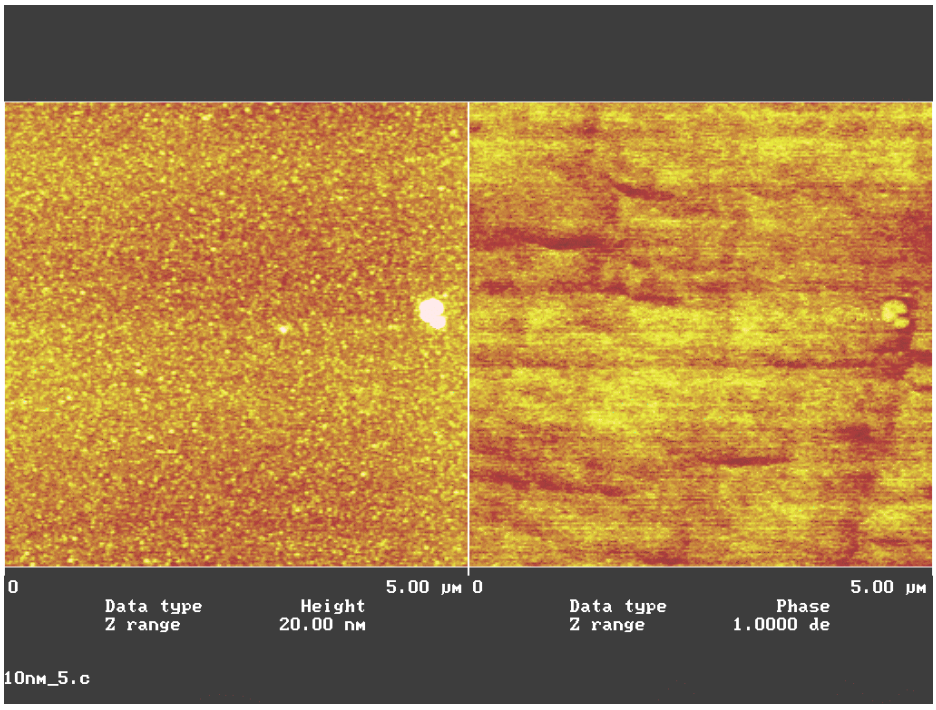


**Figure 10: 5 ìm scan of 10nm permalloy on amorphous carbon.**
**The MFM scan, on the right, shows some rippling effects, but no clear domains.**

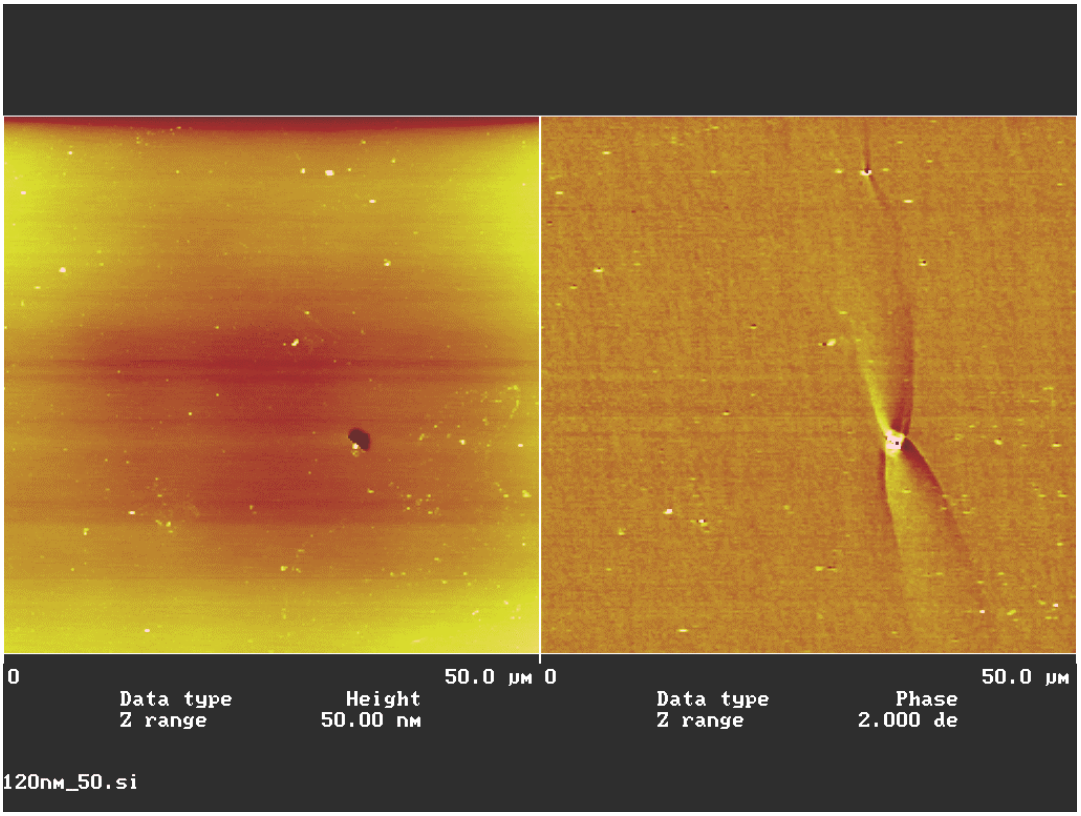


**Figure 11: 50 ìm scan of permalloy on silicon.**
**Note the bow-tie shaped domain structure on the right.**

*D. Vibrating Sample Magnetometry*

The Lakeshore Model 7300 Vibrating Sample Magnetometer located at the NASA-Langley Research Center was used to create the hysteresis loops of samples of varying thickness of carbon on silicon, permalloy on silicon, and permalloy on carbon nitride. The hysteresis loops allowed us to determine two important pieces of data: the coercivity of the sample, and the magnetization at saturation.

The coercivity was determined by measuring on the graphs (see Figures 12-14) where the magnetization returned to zero after being at negative saturation.

The saturation magnetization was also determined from these loops. The total magnetization per unit area versus thickness is reported. The area of the films were measured with a digital caliper to approximately within 2 mm.

Taking data from the hysteresis loops generated by the VSM, the average coercivity of the permalloy on amorphous carbon samples was 1.70 gauss (see Table 2). The value was higher at 2.00 gauss for the thinnest sample, with permalloy thickness of only 5nm. By contrast, the coercivity of the 120 nm of permalloy on silicon (no carbon layer) was 1.50—a difference of only 11% from the average permalloy carbon layer. Comparing equal thicknesses of permalloy on both the amorphous carbon and noncarbon sample, we find the coercivity of 120 nm or permalloy on carbon to be 1.67 gauss, and 120 nm permalloy on silicon to be 1.50 gauss: a difference of just over 10%. These results indicate that the amorphous carbon layer had only minor effects on the coercivity of the permalloy.

**Table 2: Results of coercivity vs. thickness. The coercivity is much larger for the permalloy on carbon nitride sample.**

| Thickness of permalloy (nm) | Coercive Field (gauss) |
|---|---|
| 5 | 2.00 |
| 20 | 1.67 |
| 40 | 1.50 |
| 60 | 1.67 |
| 120 | 1.67 |

| | |
|---|---|
| 120 | 1.50 |
| 120 | 14.3 |

Interestingly, the coercivity of the permalloy on carbon nitride is significantly higher at 14.3 gauss. This may indicate an effect on the quality of the thin film due to the increased roughness of the permalloy layer on CN. Taken in conjunction with the higher coercivity of the thinnest permalloy-carbon sample (5 μm permalloy) there is evidence that the structural properties may be creating a higher coercivity. The 5nm layer of permalloy will be most effected by the roughness and intermixing because these occur only in the first few monolayers. In the thicker samples there is pure permalloy above the intermixed layers.

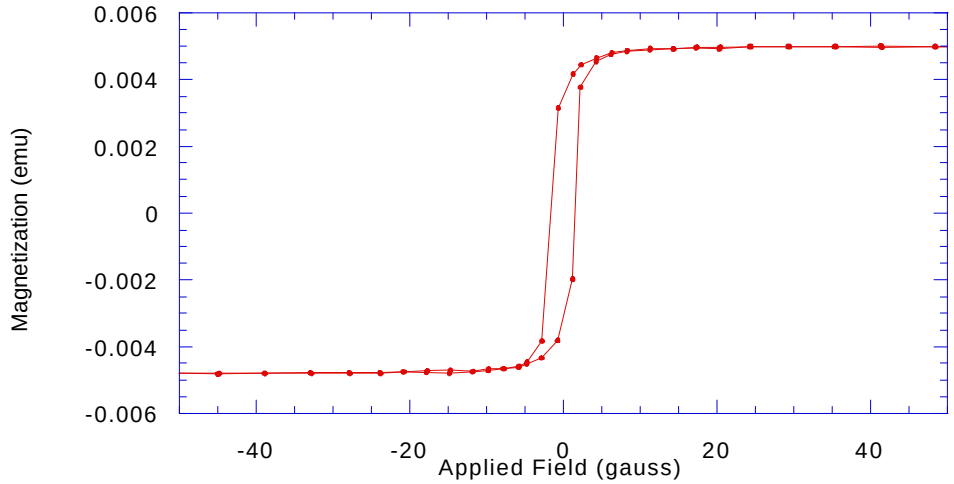


**Figure 12: Magnetization versus applied field for 120 nm of permalloy on silicon. The narrow graph indicates small coercivity.**

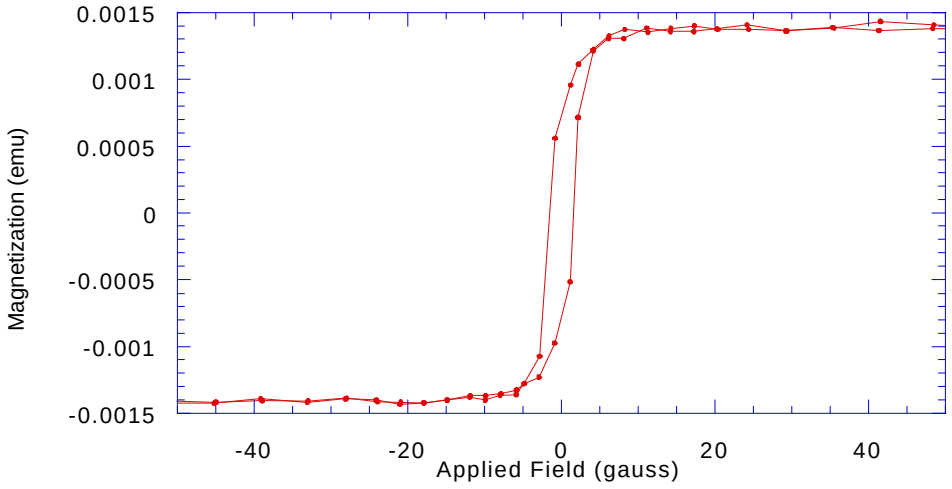


**Figure 13: Magnetization versus applied field for 60 nm of permalloy on amorphous carbon. The narrow curve indicates that this material is a good choice for sensor applications.**

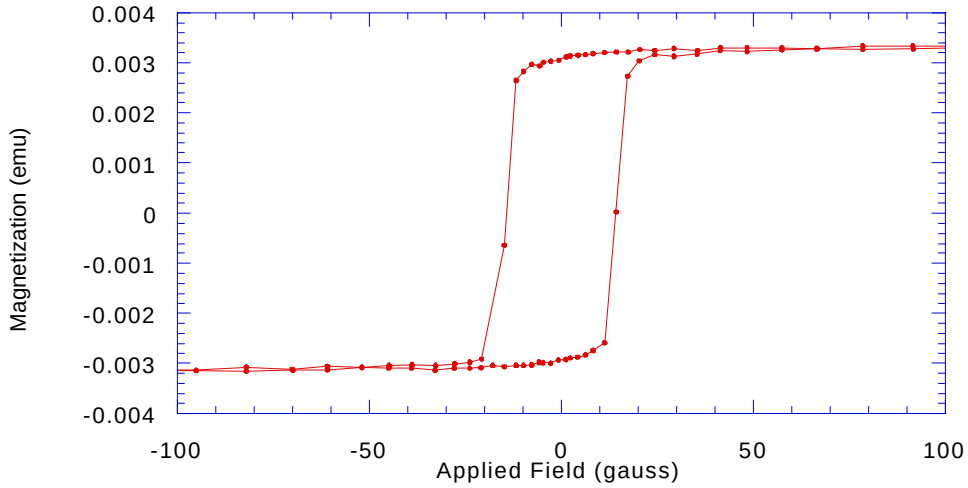


**Figure 14: Magnetization versus applied field for 120 nm of permalloy on carbon nitride. The wideness of the curve indicated increased coercivity.**

An interesting side note is that in the case of the 40 and 60 nm of carbon there seems to be a linear slope at the saturation. This seems to indicate some paramagnetic effect which we currently do not understand. This will be an area for future research to investigate. It is expected that this is not due to the carbon because carbon is diamagnetic.

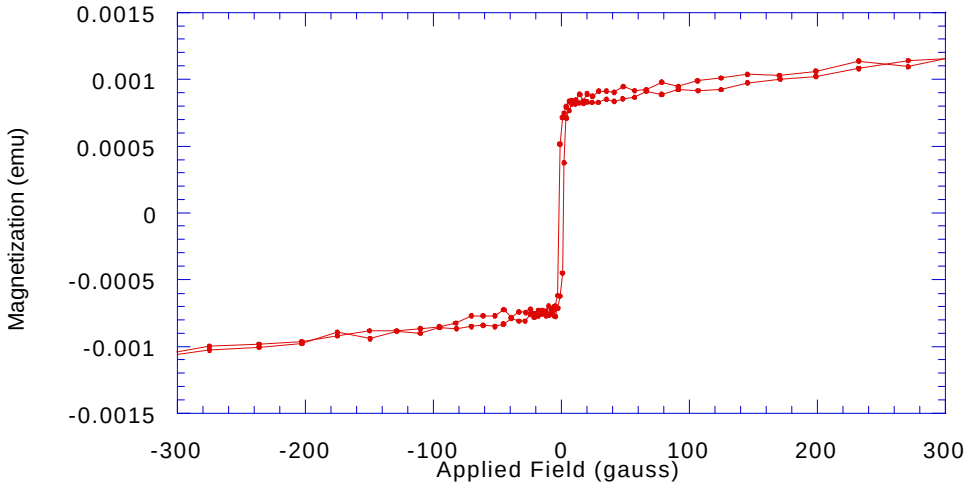


**Figure 15: Hysteresis Plot of 40 nm permalloy on amorphous carbon. Note the lineary slope at saturation. This seems to indicate presence of some paramagnetic interaction that we currently do not understand.**

The magnetization per unit area versus the thickness of permalloy was plotted to measure the effect of thickness on magnetization. We expected to see a linear relationship between thickness and magnetization given by **M**=mt, where **M** is the magnetization, m is the magnetization per unit volume, and t is the thickness. This was indeed the case.

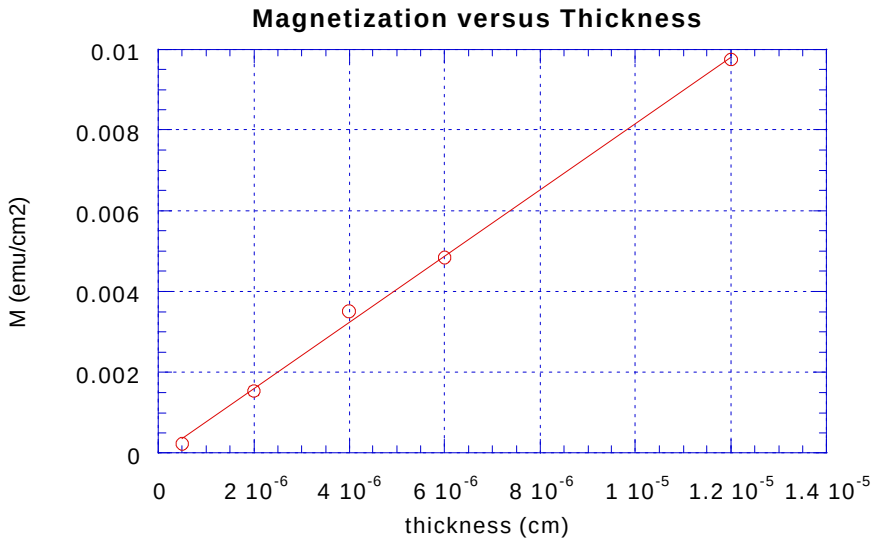


**Figure 16: Magnetization of permalloy on amorphous carbon versus thickness of the permalloy. The line is a fit to M=-6.1776e-05+822.15*t.**

The graph intercepts the y-axis at nearly zero ($-6.177 \times 10^{-5}$). The linearity of the graph and the y-intercept at zero both indicate that there is no detectable dead layer. A dead layer is a thickness with zero magnetic contribution. The slope of the graph, at 822.15 emu/cm$^3$, compares with the accepted value of 875 emu/cm$^3$, a difference of 6%.[21]

When compared with the permalloy on amorphous carbon, the permalloy on silicon sample showed a magnetization versus thickness value nearly on the same line as the other samples. Again, this indicates that the carbon had no significant impact on the magnetization. Such was not the case for the carbon nitride sample. The magnetization of the carbon nitride was far lower, at 7.64 $\times 10^{-3}$ emu/cm$^3$, than the curve ($9.56 \times 10^{-3}$ emu/cm$^3$). For the same thickness of permalloy on silicon the magnetization was 9.80 $\times 10^{-3}$ emu/cm$^3$. This too

indicates that the carbon nitride did have an impact on the magnetization of the sample.

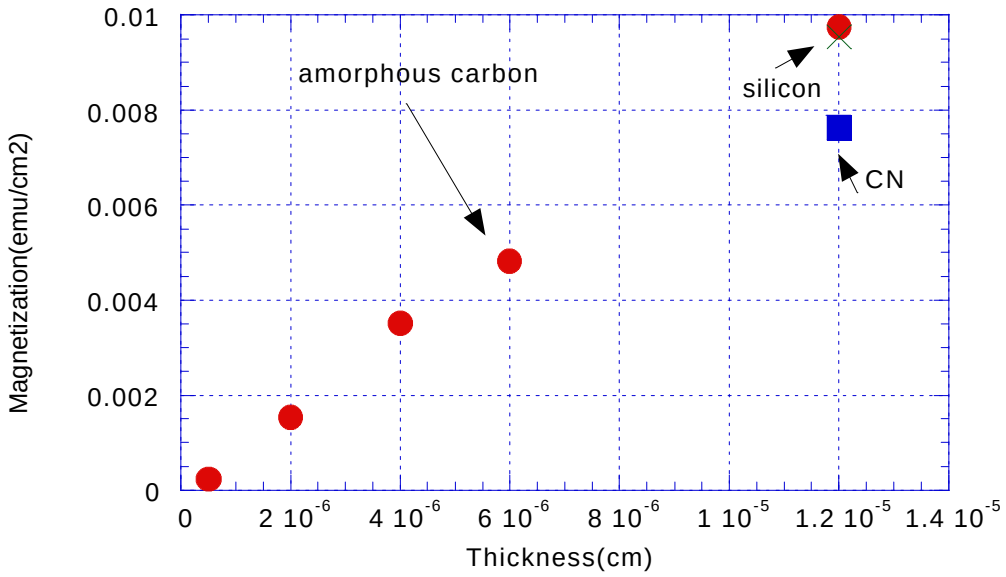


**Figure 17: Magnetization versus applied field for permalloy on various materials**

*E. Resisitivity*

Resistivity was determined by the four-point Van der Pauw method described in section III. Current was alternated from +1.0 mA to –1.0 mA five times to counteract effects due to heating. The values for the resistance are given in the following tables:

**Table2: 120 nm py on silicon. This value is slightly higher than the accepted resistivity of permalloy.**

| $R_{ab}$ (Ω) | $R_{bc}$ (Ω) | |
|---|---|---|
| *1.75* | *0.0232* | |
| *1.74* | *0.0236* | |
| *1.74* | *0.0232* | |
| *1.74* | *0.0236* | |
| *1.74* | *0.0233* | *Resistivity* |
| $<R_{ab}>$ = 1.74 | $<R_{bc}>$ = 0.0234 | *ñ= 196 Ω nm* |

**Table 3: 60 nm py on carbon. The resistivity is within the accepted range for the resistivity of permalloy.**

| $R_{ab}$ (Ω) | $R_{bc}$ (Ω) | |
|---|---|---|
| *1.91* | *0.229* | |
| *1.91* | *0.231* | |
| *1.91* | *0.230* | |
| *1.91* | *0.229* | |
| *1.91* | *0.228* | *Resistivity* |
| $<R_{ab}>$ = 1.91 | $<R_{bc}>$ = 0.229 | *ñ= 165 Ω nm* |

**Table 4: 120 nm py on carbon nitride. The measured resistance is significantly higher than the accepted value for permalloy, indicating that the carbon nitride had a significant impact on the electrical properties of permalloy.**

| $R_{ab}$ (Ω) | $R_{bc}$ (Ω) | |
|---|---|---|
| *3.67* | *0.101* | |
| *3.67* | *0.100* | |
| *3.67* | *0.101* | |
| *3.67* | *0.100* | |
| *3.67* | *0.101* | *Resistivity* |
| $<R_{ab}>$ = 3.67 | $<R_{bc}>$ = 0.101 | *Ñ= 536 Ωnm* |

**Table 5: Comparison of Resistivity Data. Note the dramatic difference between the permalloy on amorphous carbon and the permalloy on carbon nitride resistivity values.**

| Sample | Resistivity (Ù•nm) |
|---|---|
| 120 nm permalloy on silicon | 196 |
| 60 nm permalloy on amorphous carbon | 165 |
| 120 nm permalloy on CN | 536 |

The accepted value for the resistivity of permalloy is 123 +/- 40 Ù•nm[22].

The values for the permalloy in silicon and on amorphous carbon are within a

reasonable range of the accepted value. Experimental error could have occurred because of the difficulty soldering the joints. As the samples are so small, it is difficult to place the joints exactly at the edges of the surface. Van der Pauw's method requires the leads to be attached just along the periphery. Improvements in the attachments of the leads would greatly improve the accuracy of these results.

The value for the resistivity determined from the carbon nitride sample, however, is not within the range of experimental error, differing by 336% from the accepted value. We expected a higher resistivity for the carbon nitride sample because of its roughness, as indicated by the AFM scans. The increased roughness may cause more intermixing between the layers. This intermixing creates scattering sites within the conductive permalloy layer. As describes in part II, the resistivity is related to the scattering of electrons as they move through the material. The more scattering, the higher the resistance. In this light, the higher resistance of the carbon nitride is explainable and also expected.

## V. Conclusion

The results of the experiments conducted for this project clearly indicate that amorphous carbon is a good choice for the development of magnetic multilayer devices. The magnetization vs. thickness curves, the coercivity, and the saturation level of the permalloy on carbon closely resembles the results of pure permalloy without carbon. Therefore, the carbon had no negative impact on the magnetic properties of permalloy.

The carbon nitride samples offered an interesting comparison. The roughness of the carbon nitride sample, indicated by the AFM scans, probably had a significant effect on the magnetic and electrical properties of the permalloy. The total magnetization is less than that for the other samples, so for the same amount of permalloy, there was less magnetization. Also, the coercivity of the carbon nitride was increased, so it takes a larger field to flip the magnetic orientation. The roughness of the carbon nitride increased the likelihood of layer intermixing, which may have caused a dead layer to form. This dead layer decreased the magnetization of the permalloy.

Future research should focus on testing the mechanical properties of the amorphous carbon-permalloy multilayers. If these materials prove durable and inexpensive, they could be very useful to the computer industry. Also of interest would be the development of more complicated multilayers. It would be interesting to

determine whether an alternation of permalloy, carbon, and another layer of permalloy would significantly alter the magnetic properties of the device.

Further experiments should also be conducted on the development of carbon nitride multilayers. The hardness and high electrical conductivity of carbon nitride make it a very valuable material for electrical applications. However, the results of this project show that the surface must be monitored to prevent roughness and intermixing, as it diminishes both the magnetic properties and resistivity. It should be noted that one flaw in this study is that the magnetic permalloy layer had to be deposited on top of an older carbon nitride layer in a different sputtering chamber, which may have a negative impact on results. Ideally, we would like to deposit the carbon nitride and magnetic layer together at the same time in the same chamber, which will be the topic of future research. Future studies should also determine the actual amount of chemical intermixing through use of processes such as XPS.

Additionally, these initial results for the carbon nitride, with increased roughness, increased coercivity, and change in resistivity, may foreshadow some problems as harder carbon layers are attempted. It appears that the increased roughness does affect the magnetization and resistivity. This study indicates that both the benefits and detriments of this material will increase with the hardness of the carbon—a challenge to be faced when attempting to incorporate diamond-like carbon or crystalline carbon into magnetic multilayer devices.

References


[1] Gary A. Prinz, "Spin-Polarized Transport," *Phys. Today*, 58 (April 1995).
[2] Gary A. Prinz, "Magnetoelectronics," *Science*, **282**, 1660 (1998).
[3] From "The Next Step" www.nextstep.com/cgi-bin/article.cgi?file=/newmedianews/archive/1998/03/27/Tsharddisk.dtl, March 25, 2000.
[4] See 2.
[5] N. Aschroft and N. Mermim, Solid State Physics, (Philadelphia: Saunders College) 672.
[6] J.C. Anderson, Magnetism and Magnetic Materials, Chapman and Hall: London, 48-9.
[7] Richard Feynman, "Magnetic Materials," The Feynman Lectures on Physics, vol. 2, (Redwood City, CA: Addison-Wesley, 1989) 37-1.
[8] See 2.
[9] N. Ashcroft, N. Mermin, Solid State Physics,(Philadelphia: Saunders College) 721-2.
[10] Gary A. Prinz, "Magnetoelectronics," *Science*, **282**, 1660 (1998).
[11] Sean P. McGinnis, "Ion-Assisted Nucleation of Diamond Thin Films," PhD thesis, Leland Stanford Junior University, 1995.
[12] See 11.
[13] R. Krishnan, H.O. Gupta, C. Sella, and M. Kaabouchi, "Magnetic and structural studies in Ni/C,Co/C and Fe/C multilayer," JMMM,**93**, 174-178(1991).
[14] Ohanian, Modern Physics (New York: Prentice Hall, 1996), 144.
[15] See 1.
[16] E.D. Dahlberg, Jian-Gang Zhu, "Micromagnetic Microscopy and Modeling," Phys. Today, April 1995.
[17] See 15.
[18] L.J. Van der Pauw, "A Method of Measuring Specific Resistivity and Hall Effect of Discs of Arbitrary Shape" Philips Res., **13**(1958), 1.
[19] C. Merton, G.D. Skidmore, J. Schmidt, E.D. Dahlberg, " Magnetic Reversal of Tapered Permalloy Bars With Holes in the Center," J. Appl. Phys., **85,** 4601 (1999).
[20] See 18.
[21] Richard Bozorth, "Ferromagnetism," IEEE, 1993.
[22] A.C. Reilly, W. Park, R. Slater, B. Ouaglal,R. Loloee, W.P. Pratt Jr., J. Bass, "Perpendicular Giant agnetoresistance of Co91Fe9/Cu Exchange-Biased Spin-Valves: A Further Test of the Unified Picture,"JMMM, **195**, L269-L274 (1999).